

ASSIMILATION IMPACTS OF AMSU SNOW/ICE EMISSIVITY MODEL IMPROVEMENTS

Kozo Okamoto<sup>1</sup>, John Derber<sup>2</sup>, Banghua Yan<sup>3</sup>, Fuzhong Weng<sup>4</sup>, Xingren Wu<sup>5</sup>

<sup>1</sup>NOAA/NWS/NCEP/EMC, UCAR, JMA, Camp Springs, Maryland

<sup>2</sup>NOAA/NWS/NCEP/EMC, Camp Springs, Maryland

<sup>3</sup>QSS Group Inc, Camp Springs, Maryland

<sup>4</sup>NOAA/NESDIS/ORA/JCSDA, Camp Springs, Maryland

<sup>5</sup>NOAA/NWS/NCEP/EMC, SAIC, Camp Springs, Maryland

1. INTRODUCTION

Radiance data from the Advanced Microwave Sounding Units - A (AMSU-A) and - B (AMSU-B) onboard the National Oceanic and Atmospheric Administration (NOAA) satellites are extremely important for operational data assimilation. The National Centers for Environmental Prediction (NCEP) has operationally assimilated AMSU-A/B radiances from the NOAA 15, 16 and 17 satellites in its Global Data Assimilation System (GDAS) with the Spectral Statistical Interpolation (SSI) system. When all three instruments were functioning, the data from these three satellites provided almost complete global coverage over the six hour assimilation time window.

However, few window and lower-tropospheric sounding channels are used over the sea-ice and snow conditions because of difficulty in estimating the surface emissivity and the surface temperature required by the radiative transfer calculations. Since in the polar region in-situ measurements are sparse, improved use of AMSU radiances can potentially generate substantial impact on the numerical weather prediction (NWP). This paper presents the analysis and forecast impacts from the use of a new snow/ice microwave emissivity model.

2. Emissivity model

The current microwave emissivity model for snow, desert and vegetation surfaces embedded in the SSI is based on Weng et al. (2001). It calculates a volumetric scattering using a two-stream radiative transfer approximation to estimate the surface emissivity for the frequency range from 4.9 to 94.0 GHz. This model has successfully produced reasonably accurate microwave emissivities over many areas, but at frequencies higher than 80GHz and over various snow types it has not produced sufficiently accurate results. In addition, the sea-ice emissivity is inadequate being fixed at 0.92 for all frequency ranges.

Yan et al. (2004) has developed a statistical approach for estimating the snow/sea-ice microwave emissivity, based on the ground-based measurements and the satellite retrievals. This model uses an emissivity data set based on 16 snow types over the frequency range of 5 to 200 GHz. The snow type is identified using the surface temperature and the

observed brightness temperature of window channels. The emissivity is then determined using the predefined emissivity data set and interpolating to the appropriate frequency. The data set is shown in Fig.1 for the 16 snow types. Details of the new snow emissivity model can be found in Yan et al. (2004). Sea ice emissivity is similarly determined by using surface temperature, observations and sea-ice emissivity data set.

3. Analysis Impacts

In the satellite data assimilation system, the brightness temperatures are simulated using a fast radiative transfer model and surface emissivity model from the analysis variables and compared to the actual observations. The model variables are then adjusted based on the differences between all the simulated and observed quantities and the appropriate error statistics to produce the most probable atmospheric state. Therefore, to evaluate the impacts of the improved new snow/ice microwave emissivity model, we first focus on the difference between simulated and observed brightness temperatures. The simulation is performed using an operational radiative transfer model using transmittances calculated with OPTRAN (Kleespies et al. 2004), and a first-guess (3,6,9-h forecasts interpolated to the observation location) from GDAS. This difference, G-O, is also an important parameter in quality control procedures in the SSI. We conducted two T62L28 assimilation cycle runs (one

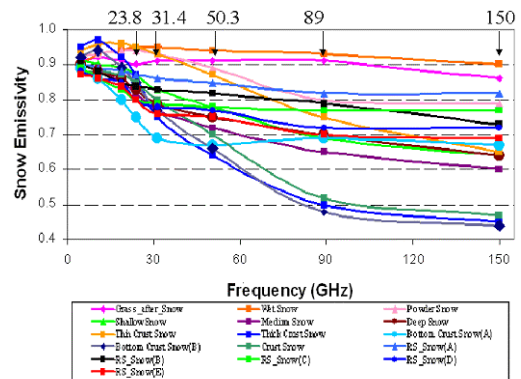


Fig.1: The emissivity spectra between 5 and 150 GHz for 16 snow types, used in the new microwave emissivity model.

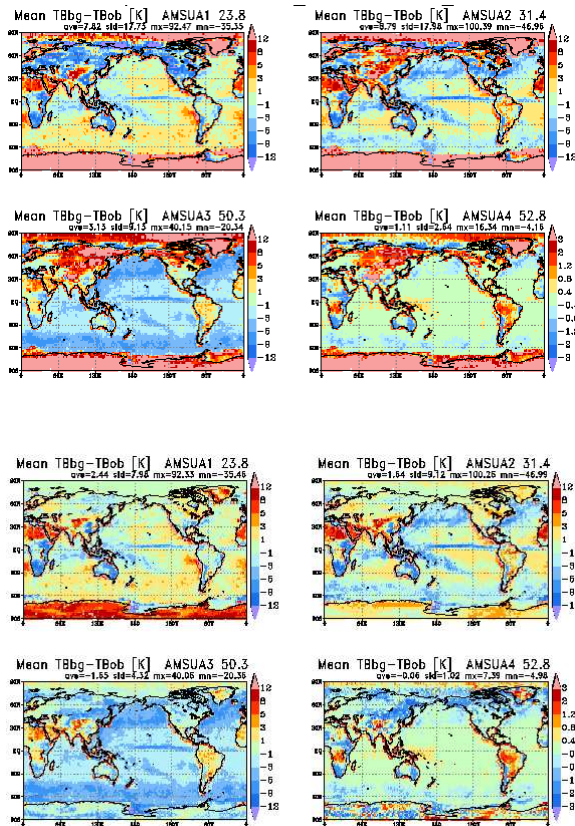


Fig.2: The mean of simulated – observed brightness temperatures for AMSU-A1 to –A4 from NOAA16 averaged over 2x2 degree grid boxes from 00 UTC 2 to 18 UTC 31 December 2003. Upper four panels are from the current microwave emissivity model, lower panels are from the new model.

with the new microwave emissivity model and the other with the current emissivity model) for one month of December 2003 to investigate G-O statistics.

Fig.2 shows monthly mean G-O of AMSU-A channels 1, 2, 3 and 4 from NOAA16 for 2 x 2 degree boxes with the current model (upper four panels) and with the new emissivity model (lower four panels). The new emissivity model substantially reduces the mean G-O difference. Relatively large differences remain in Greenland and Antarctica. This is probably associated with the poor estimate of the surface temperature caused by the inconsistency between the real elevation and GDAS model elevation.

Table.1 shows the difference of monthly G-O rmse for AMSU-A channels 1–6, 15 and AMSU-B channels 1-5 from NOAA16 for 2 x 2 degree boxes at latitude bands of 50N-90N and 50S-90S. Negative values indicate the new emissivity model reduces G-O rmse compared with the current emissivity model. The rmse is clearly reduced for all channels but AMSU-B channel 3 (AMSU-B channel 3 primarily measures the middle to upper tropospheric water vapor in mid- or low- latitudes.)

Because the SSI rejects radiances with large G-O and also adjusts the observation weight based on G-O, the reduction in G-O by the new emissivity model can make more radiance data available with greater weights. Table 2 shows average numbers used for a single SSI analysis for AMSU-A and –B in high latitudes of both hemispheres. The numbers of available data with the new emissivity model grows by a factor of 1.2 to 3.3 for AMSU-A and 1.3 to 2.0 for AMSU-B. A clear change is not seen for AMSU-A channels 7-14 whose weighting functions peak above 250 hPa.

Fig.3 shows the zonal mean temperature analysis difference at 00 UTC on 31<sup>st</sup> December 2003. The use of the new emissivity model and the resulting additional data produce an increase in the lower tropospheric temperature in the northern polar region. This increase in lower tropospheric temperature indicates that these observations may be correcting a low-temperature bias of the forecast model. It should be noted that the impact, also occurring at the first analysis of the assimilation cycle (not shown), is localized to latitudes poleward of 60-degree and does not substantially propagate to lower latitudes.

#### 4. Forecast impacts

To assess the impacts on the forecasts, we conducted fully cycled assimilation experiments with higher vertical resolution system, T62L64, for January 2004. The results from the run with the current emissivity model, “Control”, and the new emissivity model, “Test1”, are depicted by black and red lines respectively in Fig. 4. The impact for the whole hemisphere (20N-80N/20S-80S) are neutral or slightly positive in terms of the 500Z anomaly correlations (ANC, Fig.4 (a) and (b)), as expected from localized results shown in Fig.3. Focusing on the polar region (60N-90N/60S-90S), obvious impacts are not still found for 500Z ANC (Fig.4(c) and (d)). In contrast,

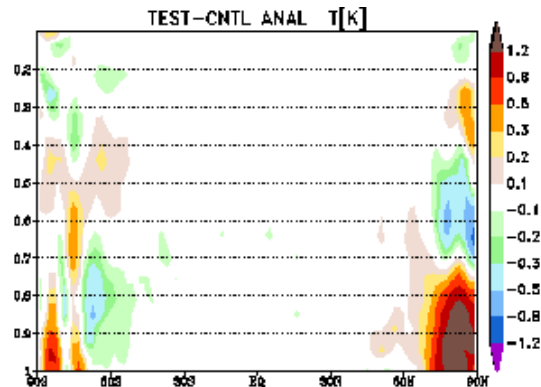


Fig.3: The zonal mean difference between the analyzed temperature using the new and current microwave emissivity model at 00 UTC on December 31, 2003. This is 31<sup>st</sup> day of the assimilation experiment. .

Table.1: The difference of the rmse differences in simulated-observed AMSU-A and -B brightness temperatures from NOAA16 between using the new emissivity model and current model. The rmse is calculated from all data in latitudes of 50N-90N/50S-90S during the same period in Fig.2. Negative values indicate that the new emissivity model produces smaller rmse differences.

|         | AMSU-A1 | AMSU-A2 | AMSU-A3 | AMSU-A4 | AMSU-A5 | AMSU-A6 | AMSU-A15 |
|---------|---------|---------|---------|---------|---------|---------|----------|
| 50N-90N | -9.46   | -11.96  | -5.55   | -0.58   | -0.07   | -0.04   | -19.15   |
| 50S-90S | -20.87  | -22.58  | -9.00   | -2.63   | -0.58   | -0.03   | -11.22   |

|         | AMSU-B1 | AMSU-B2 | AMSU-B3 | AMSU-B4 | AMSU-B5 |
|---------|---------|---------|---------|---------|---------|
| 50N-90N | -15.42  | -13.71  | 0.05    | -0.24   | -3.59   |
| 50S-90S | -9.83   | -9.08   | 0.08    | -0.19   | -3.31   |

Table.2: Average number of data used in a single analysis. Averages produced over same period as in Fig. 2..

|         |         | AMSU-A1 | AMSU-A2 | AMSU-A3 | AMSU-A4 | AMSU-A5 | AMSU-A6 | AMSU-A15 |
|---------|---------|---------|---------|---------|---------|---------|---------|----------|
| current | 50N-90N | 251.8   | 285.0   | 306.3   | 311.2   | 311.4   | 464.8   | 225.5    |
| New     |         | 831.7   | 885.8   | 912.1   | 928.3   | 935.1   | 1246.4  | 424.4    |
| current | 50S-90S | 703.7   | 758.1   | 776.6   | 777.3   | 777.5   | 953.6   | 612.3    |
| new     |         | 860.6   | 994.2   | 1019.0  | 1026.5  | 1039.8  | 1294.5  | 746.1    |

|         |         | AMSU-B1 | AMSU-B2 | AMSU-B3 | AMSU-B4 | AMSU-B5 |
|---------|---------|---------|---------|---------|---------|---------|
| current | 50N-90N | 112.5   | 113.9   | 113.9   | 113.9   | 113.9   |
| New     |         | 220.3   | 221.8   | 221.8   | 221.8   | 221.8   |
| current | 50S-90S | 239.0   | 243.5   | 243.5   | 243.5   | 243.5   |
| new     |         | 304.4   | 308.7   | 308.7   | 308.7   | 308.7   |

the rmse in 850T is reduced (Fig.4(e)), while a negative bias is larger (Fig.4(f)). This bias increase is associated with a negative lower-tropospheric temperature bias in the polar region from the forecast model. Because the newly introduced AMSU radiance data increases the lower-tropospheric polar temperatures and the forecast model decreases the temperatures results in the apparent bias since these scores are validated against their own analysis.

The behavior of this polar temperature change in the new analysis agrees with sensitivity experiments of a newly developed sea-ice model in the forecast model. This sea-ice model is based on Winton's (2000) three-layer thermodynamic process. The heat and moisture fluxes, and albedo are treated separately for the ice and open water, but assumed well mixed in the air (Wu et al. 1997).

The impact of coupling the new microwave emissivity model in the SSI with the new sea-ice model in the forecast model has also been examined. The results of this new experiment, "Test2", are shown by green line in Fig.4. Overall, the Test2 run generates slightly greater positive impacts than the Test1 run and the Control run, substantially decreasing the negative bias even compared with the Control run.

## 5. Conclusions

A new microwave emissivity model for the snow/ice surface substantially decreases the

differences in the brightness temperature between the observations and simulations, allowing many more window and lower tropospheric radiance data to be used in the polar region. This generates an analysis which has a substantially warmer, less biased, polar lower-tropospheric temperature. The impacts on the forecast skills are small but positive in the reduction in rmse of 850T. The bias in the lower tropospheric forecast temperature, which is apparently increased by the new emissivity model, is reduced by coupling the emissivity model in the analysis with a new sea-ice model in the forecast model.

We plan to conduct further impact assessments of the coupled system for longer periods and different seasons. In addition, the use with polar winds derived from the Moderate Resolution Imaging Spectroradiometer (MODIS) also addresses the data sparsity problem in the polar region. Experiments examining the relative impacts of the improved emissivity and the use of the MODIS winds are underway. Preliminary experiments showed contributions by both changes with slightly more impact from the new emissivity model (Jim Jung 2004, personal communication).

## References

Kleespies, T. J., P. V. Delst, L. M. McMillin, and J. Derber, 2004: Atmospheric Transmittance of an Absorbing Gas. 6. OPTRAN Status Report and

Introduction to the NESDIS/NCEP Community Radiative Transfer Model, *Applied Optics*, **43**, 3103-3109

Weng, F., B. Yan, N. C. Grody, 2001: A microwave land emissivity model, *J. Geophys. Res.*, **106**, 20,115-20,123

Winton, M., 2000: A reformulated three-layer sea ice model, *J. Atmospheric and Oceanic Technology*, **17**, 525-531.

Wu X., I. Simmonds, and W. F. Budd, 1997: Modeling of Antarctic sea ice in a general circulation model, *J. Climate*, **10(4)**, 593-609

Yan, B., F. Weng, K. Okamoto, 2004: Improved Estimation of Snow Emissivity from 5 to 200 GHz, *submitted to IEEE Transactions on Geoscience and Remote Sensing*.

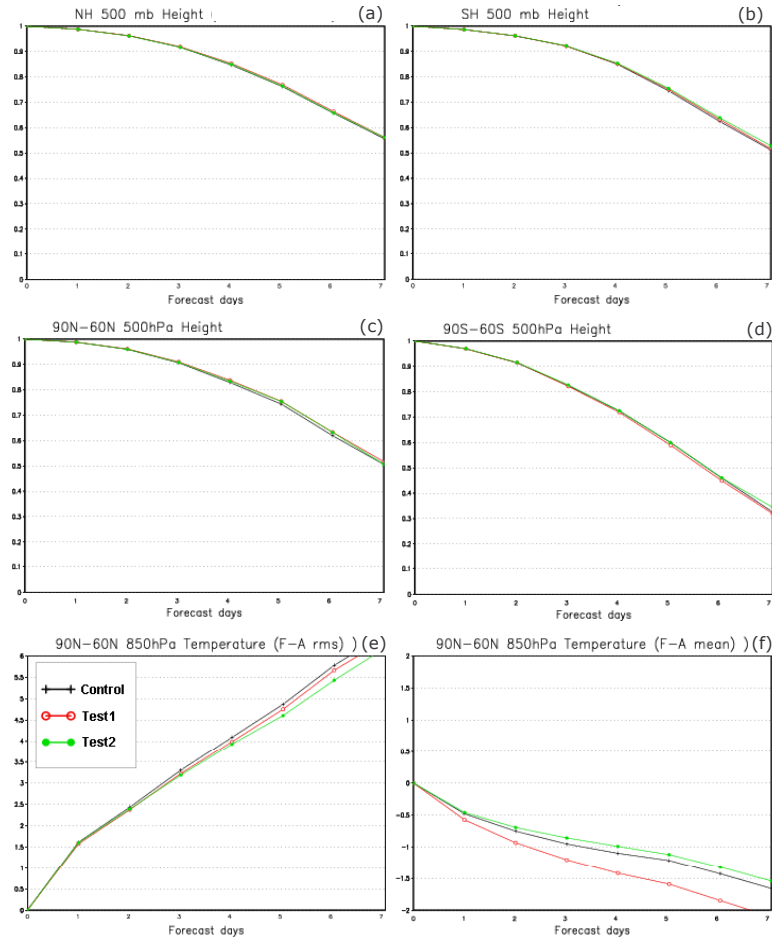


Fig.4: Forecast skills for the Control run (black), Test1 run with new microwave emissivity model (red), and Test2 run with new emissivity model and sea-ice model (green). (a)-(d): 500Z Anomaly Correlation (ANC) for the 20N-80N, 20S-80S, 60N-90N and 60S-90S, respectively, (e): 850T rmse